Data Repository Item 2003044: Table DR1: Abundance, concentration, and sizes of quartz and zircon phenocrysts

Tuff Sample	unit	pre-eruptive T (Qz-Mt) T °C	Zrc sat T °C	Crystal content vol%	Concentration SiO2 wt%	Zr ppm	Abundance Qz vol%	Zrc ppmv	n Qz cm^{-3}	n Zrc cm^{-3}	Mean size Qz um	Mean size Zrc um	Median size Qz um	Median size Zrc um	Measured number Qz	Measured number Zrc
Lower Bandelier (LBT), Toledo Caldera, NM, 600 km³ , 1.61 Ma																
LBT-10	Late	771		25	75		8.7		77		1156		1070		159	
LBT-4	Early	737		10	77		4.4		1129		326		265		242	
Bishop (BT), Long Valley Caldera, CA, 650 km³ , 0.76 Ma																
LV-27	Early	714	735	9	78	89	3.8	12	66	28	830	94	757	89	138	500
BC97-16	Early	754	735	9	78	89	2.1		73		738		635		179	
LV-751	Late	762	761	15	76	118	6.4	16	98	37	1084	88	1044	79	110	367
LV-748	Late	817	776	13	73	140	5.8	17	85	67	1164	99	1072	94	156	352
LV-3	Late	763	767	27	73	138	11.8	27	132	98	1110	78	1036	72	180	614
LV-13	lava		801	15	72	200	1.6	51	42	345	724	35	617	26	111	544
Lava Creek (LCT), Yellowstone Caldera, WY, 1000 km³ , 0.64 Ma																
LCT-3a, A	Early	800	809	11	78	187	7.8	14	780	37	472	95	380	89	318	304
LCT-4, B	Late	912	863	22	74	365	16.4		162		1099		1043		163	
YL-4	lava		882	9	76	393	2.0	70	61	325	343	84	297	80	238	430
Huckleberry Ridge(HRT), Big Bend Caldera, WY, 2500 km³ , 2.04 Ma																
HRT-3a, A	Early		863	19	77	328	9.8	25	113	108	1054	76	1019	59	257	342
HRT-1, B	Late		868	26	74	399	12.1		179		952		863		211	
HRT-C, C	Late		897	21	75	445	8.2	33	185	114	874	95	797	88	283	343
Mesa Falls (MFT), Island Park Caldera, ID, 300 km³ , 1.3 Ma																
MFT-1			800	37	78	168	18.5	49	88	41	1387	128	1302	114	283	307
Ammonia Tanks (AT), Timber Mountain Caldera, NV, 1000 km³ , 11.45 Ma																
TM-15	Early	762	809	14	76	215	7.0	22	83	67	948	84	757	76	206	637
TM-17	Late	870	842	20	73	293	2.9	16	171	47	617	77	565	71	209	508
TM-24	lava	754	776	7	76	135	2.3	8	241	125	486	42	437	37	167	160
Katmai-Valley of 10,000 Smokes rhyolite, AK, 8-12 km³ ,1912 AD																
KTM-3	Early		790	2	77.4	158	0.9		83		525		523		238	
Novarupta	Late	949	786	2	76.6	157	0.5		87		592		430		241	
Yongest Toba Tuff, Toba Caldera, Indonesia, 2800 km³ , 0.074 Ma																
YTT-102	Early	752	762	27	75.6	107	8.8	28	43	96	1150	75	940	69	166	404

*Oxygen isotope T (°C) estimates and sample descriptions are from Bindeman and Valley (2001, 2002)

n-measured particulate abundance (Fig. 1-2) per 1cc of melt; no zircons are found in Katmai samples, suggesting Tmagma>TZrc sat

Data Repository Item 2003044: Appendix

Methods

Individual pumice clasts (weighing between 20 and 1000 g) were collected from early and late erupted portions of stratigraphically-defined ignimbrites and fall units of several well-studied large volume ash-flow tuffs, and vesicular glassy samples of smaller volume lavas (Table DR1). The studied samples are low-to high-silica rhyolites with high-silica rhyolitic vesicular groundmass.

Acid dissolution. Pumice clasts were dissolved in 30-48% HF, or less reactive fluoroboric acid (HBF_4) (Line and Aradine, 1937). For quartz extraction, the total time of HF reaction with 200 g of lightly-crushed vesiculated pumice did not exceed 5-10 minutes. Reaction yielded phenocrysts in residue at the bottom of the teflon beaker and these were washed with distilled water, alcohol, and dried at 110°C. Optical and SEM examination of phenocrysts was performed following dissolution (Photo Collage Fig. DR1). Feldspar phenocrysts show significant etching, less intense etching and breakage characterizes biotite, amphibole, pyroxenes, and magnetite (but not ilmenite) crystals (see also Hones, 1927). Phenocrysts of quartz and zircons show no evidence of dissolution, and no difference between HF-, and HBF_4-extraction of quartz was observed. Even the smallest quartz crystals (100μm) show insignificant etching after 1 hour in HF (Fig. DR1, last image). Dissolution enables measurements of weight and volume proportion of crystals (Table DR1), defined as weight of extracted crystals/weight of rock, corrected for mineral/rock density ratio.

Sources of error. The main source of error in zircon extraction using acid is crystal attachment to teflon beaker and to Petri-dish owing to static electricity and surface tension. The relative errors could be large when zircon concentration is small (e.g., 1-2 mg per 100g of rock). A test estimated % loss of zircon during transfer from a series of 2 teflon beakers to a final Petri dish. The weight and CSD of the initial and final population were measured. The CSD shape is preserved within error, the retrieved mass decreased by 0.3-0.5 mg. Therefore for a typical 5-10 mg population of zircons the error in zircon volume proportions (Table DR1) is ±5-10%.

CSD Measurements. A Scion-NIH Image program and a camera attached to a microscope were used to make a series of photo images of extracted phenocrysts, and to measure their length, width, and area. The volume of each crystal was calculated, as a sphere (quartz), or prism (zircons), and only whole crystals and crystals that constitute larger part of whole crystals were selected and measured for CSD. Between 150 to 400 crystals of quartz, and 250 to 700 crystals of zircon were measured in each sample (Table DR1). It is necessary to separate touching crystals (either on a glass slide, or on the image), and successfully threshold the image prior to making computer-assisted measurements. Scion-NIH Image program automatically calculates length, width, area and other parameters in pixels. In is necessary to convert pixels into millimeters or microns at given magnification. Data collected in the Scion-NIH Image program is exported to Excel for further calculations (see below), and results are plotted in any graphic program (e.g. KaleidaGraph).

The particle concentration can be determined through:

1) calculating the volume of N crystals measured for CSD:

$$V_N = \sum_{i=1}^{i=N} (LW^2) \quad \text{for 4-sided prismatic zircons}$$

$$V_N = \sum_{i=1}^{i=N} (4/3\pi R^3) \quad \text{for spherical quartz}$$

where L, W, and R are measured length, width, and radius of each crystals;

2) calculating the weight of these N crystals by multiplying V_N by crystal's density: 4.6 g/cm^3 for zircon and 2.65 g/ cm^3 for quartz;
3) calculating what fraction does the V_N constitute from the total weight of extracted zircon or quartz (per starting weight of a rock);
4) calculating particle concentration per 1 cm^3 of rock, and after making a small adjustment for other crystals present (rock crystallinity, typically 5-20%), particle concentration per 1 cm^3 of melt, as is given

in Table DR1. The latter parameter allows construction of volume-normalized log-linear CSD diagrams on Fig. 1 (text). It also allows calculation of mean distance between crystals in a melt (not plotted). Normalization to 1 cm^3 rather than 1 mm^3 (which are commonly used in converting thin section 2D data into volume) helps better visualization, and is more appropriate for 1-mm phenocryst sizes at measured particle concentrations.

Plotting data. The log-linear plots (Fig. 1 text) and volume normalization procedures are commonly employed (e.g. Cashman and Marsh 1988; Marsh 1988; 1998; Higgins 1998), and the y-axis has dimension of cm^{-4}. This is because in addition to volume-normalization (cm^{-3}), the number of crystals of certain size is also normalized (divided) by the bin width used: 0.001 cm (10μm) for zircon, and 0.02 cm (0.2mm) for quartz. Such normalization yields dimension of cm^{-4}, and makes histograms insensitive to variation in bin widths.

Log-linear coordinates (Fig. 1, text), and normalization to volume, have kinetic significance. It has been shown for many systems, such as in "industrial crystallizer" (e.g. Lasaga 1998) and in some open system, predominantly mafic subvolcanic magma bodies (Cashman and Marsh 1988; Marsh 1998) that exponentially increasing nucleation with time yields linear arrays in these coordinates. Readers are referred to Randolph and Larson (1988); Cashman and Marsh (1988); Marsh (1988; 1998), Lasaga (1998), and Eberl et al. (1998, Amer Mineralogist 87: 1235-1241, 2002) for the relevant discussion of applicability and limitations of such diagrams. For the purpose of this study, the normalized diagrams (Fig. 1) can be treated as histograms of abundance that correctly identify relative proportions of crystals.

It is important to note that the observed deficiencies of small crystals on the left-hand side of CSD plots do not result from any stereological corrections, such that result from transforming two-dimensional thin section measurements into three dimensions (e.g. Higgins, 1998 and references therein). The present work does not rely on any stereological correction. Lack of smallest crystals of quartz, smaller than a threshold size (<0.1 mm) was independently confirmed by examining thin sections of pumice clasts and welded ignimbrite from Bishop Tuff, Lava Creek Tuff, and Huckleberry Ridge Tuff, and in a Lava Creek Tuff sample LCT-3a crushed by an electric pulse disintegrator technique at 100kV (e.g. Rudashevsky et al., 1995) that preserves crystal morphologies.

Advantages. Acid dissolution of pumice clasts is a successful and a relatively simple method to extract intact population of acid-resistant minerals such as quartz and zircon, and to measure their abundance, sizes and CSDs. The main advantage of dealing with acid-extracted and intact crystal populations, is that no surface/volume and shape-factor correction (e.g. Higgins 1998) are needed as crystals are extracted quantitatively and three-dimensional shape is measured. Recently, a non-destructive method of mineral separation by electric pulse disintegration at 100 kV discharge has been proposed (Rudashevsky et al., 1995). This method is promising for extraction of intact zircon and quartz populations from plutonic (and metamorphic) rocks for CSD study that would be difficult to achieve using the acid extraction technique outlined here. Acid dissolution works best for glassy vesicular samples that react quickly and yield quantitative populations in residue.

Relevant references

Acid extraction and etching:

Line, W.R., Aradine P.W. (1937) Determination of quartz in the presence of other silicates. Industrial Engineering Chem Anal Ed. V. 9, p. 60-63.

Hones A.P., (1927) The nature, origin and interpretation of the etch figures on crystals. John Wiley and Sons, New York, 172 p.

Alternative method for non-destructive mineral separation using electric-pulse disintegration:

Rudashevsky, N.S., Burakov, B.E., Lupal, S.D., Thalhammer, A.R., and Saini-Eidukat, B., 1995, Liberation of accessory minerals from various rock types by electric-pulse disintegration-method and application, Transactions of the Institution of Mining and Metallurgy, v. 104, p.C25-29.

Other methods that have produced concave-down CSDs in zircons, apatites, and magnetites

A) Measured in thin sections in migmatites and granites:

List, F.K.,1966. Statistical investigation of zircon and apatite in anatexites of the southern Bavarian complex Geologische Rundschau. V. 55, p. 509-530.

Kraus, G., 1962, Gefuge, Kristallgrossen and genese des kristallgranites I im volderen Bayerischen Wald: Neues Jahrbuch fur Mineralogie Abhandlungen, v. 97, p. 357-434.

Nemchin, A.A., Giannini, L.M., Bodorkos, S., and Oliver, N.H.S., 2001, Ostwald ripening as a possible mechanism for zircon overgrowth during anatexis: Theoretical constraints, a numerical model, and its application to pelitic migmatites of the Tickalara Metamorphics, northwestern Australia: Geochimica et Cosmochimica Acta, v. 65, p. 2771-2788.

B) Measured by magnetic methods:

Latham, A.G., Harding, K.L., Lapointe P., Morris, W.A., Balch, S.J., 1989. On the lognormal distribution of oxides in igneous rocks, using magnetic susceptibility as a proxy for oxide mineral concentration: Geophysical Journal, v. 96, p. 179-184.

Breakage and lognormality

It has been shown, and mathematically proven that breakage of particles asymptotically yields lognormal distribution (Kolmogorov, 1941; Epstein, 1947; Mahmood, 1973)

Kolmogorov, A.N., 1941. On lognormal distribution law of dimensions of particles under crushing: Doklady of the Academy of Sciences of the USSR, 31, p. 99-102.

Epstein B., 1947. The mathematical description of certain breakage mechanisms leading to the logarithmico-normal distribution: Journal of the Franklin Institute, v. 244, p. 471-457.

Mahmood, K., 1973. Lognormal size distribution of particulate matter: Journal of Sedimentary Petrology, v. 41, p. 1161-1166.

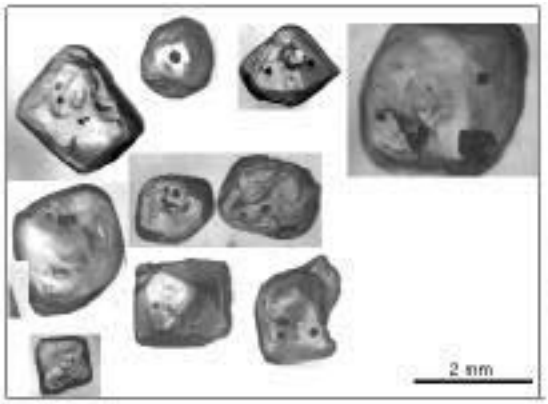

Late Bishop Tuff, HBF4 extracted quartz from a single pumice clast LV-03

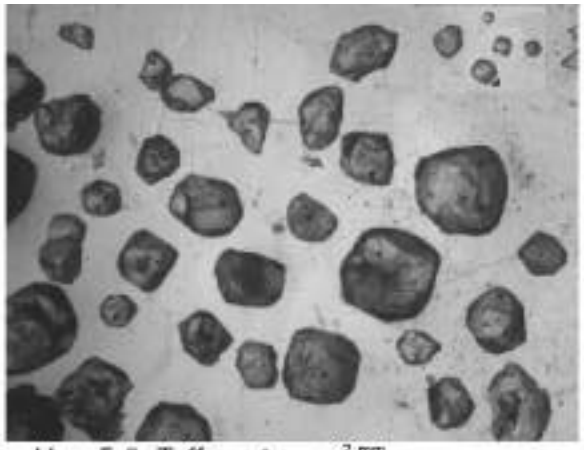

Mesa Falls Tuff quartz 2 mm

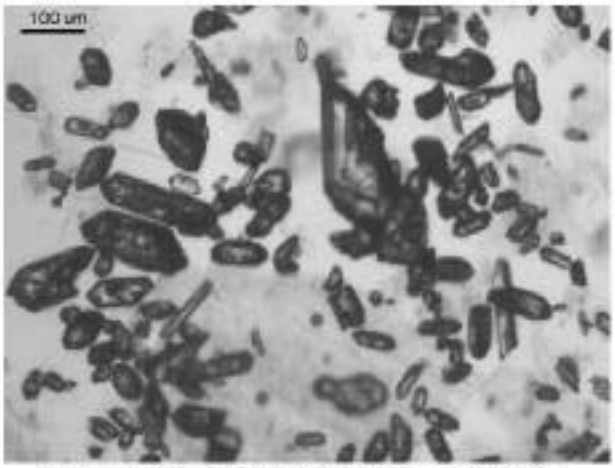

Post-Caldera small volume intracaldera dome Long Valley, LV-13; zircons range in age in shape but show steep CSD (Fig. 1B)

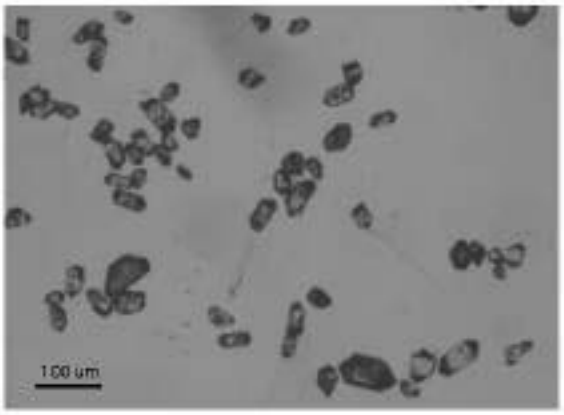

Lava Creek Tuff Member A, HF-extracted zircons

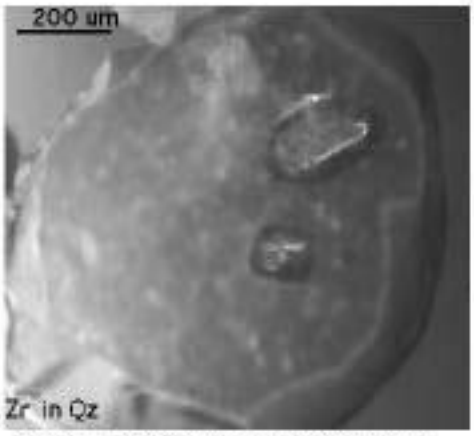

YL-4, Dunraven Rd Flow, Yellowstone Quartz phenocryst with large zircons

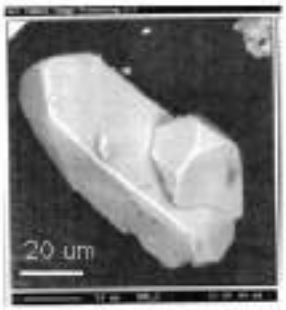

SE image of rare zircon twin sample YL-4

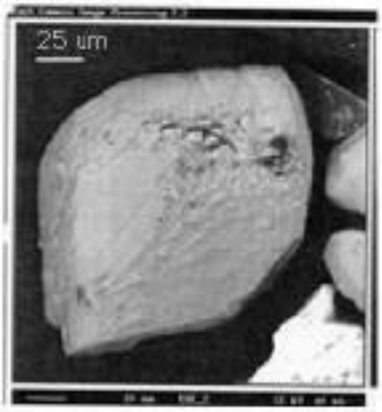

Partially etched smallest quartz after 1 hour in HF, SE image sample YL-4

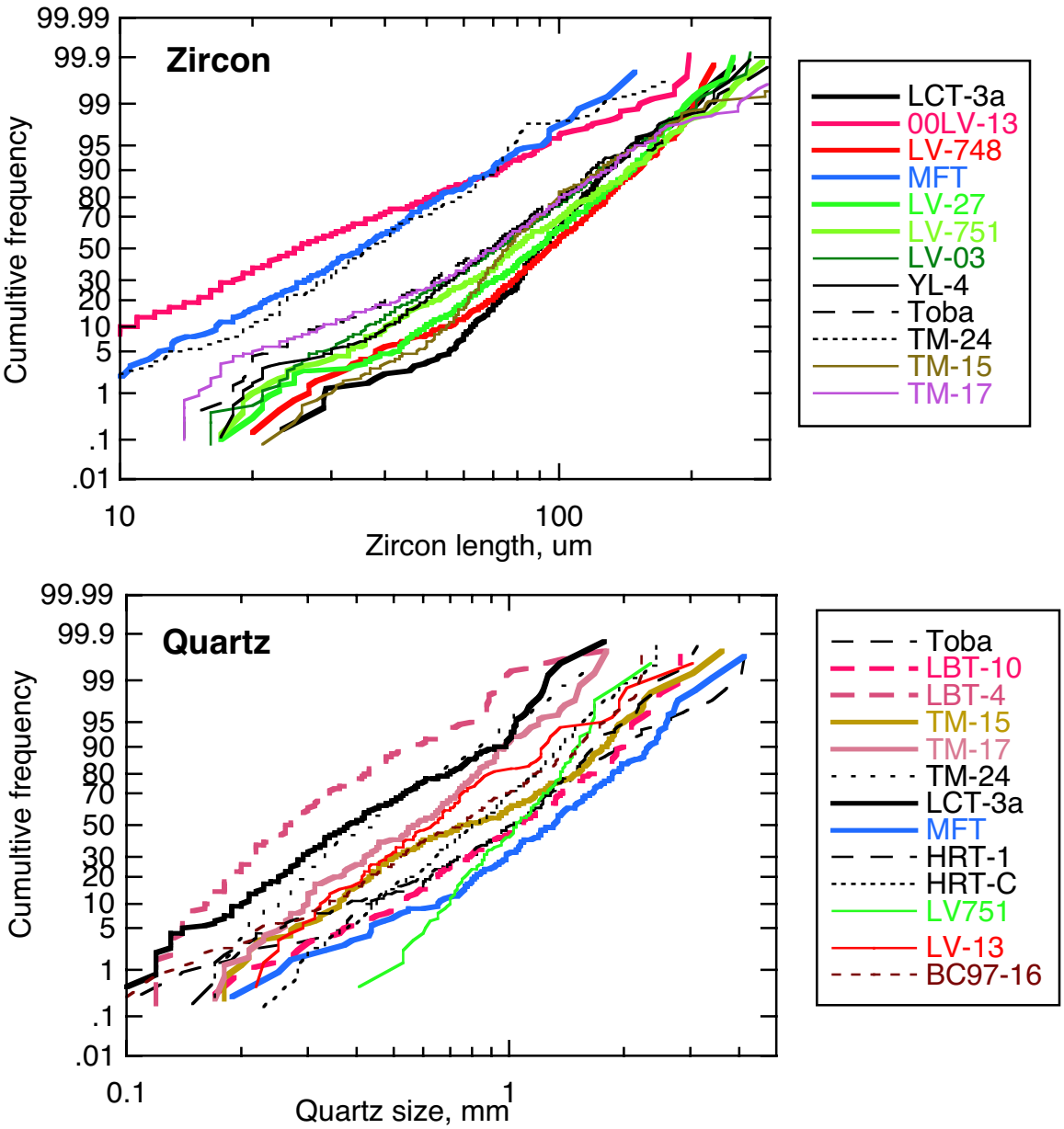

CSD of quartz and zircon best approximate straight line that suggest lognormality in these coordinates (Crow and Shimizu, 1988). Other tests (Smirnov-Kolmogorov and $\chi 2$) suggest lognormality as well (see text for discussion and Table 1 for samples).